An explanation for deviations from the quark number scaling of elliptic flows in low p_T region*

YAO Tao(姚涛)[1;1)] XIE Qu-Bing(谢去病)[1] SHAO Feng-Lan(邵凤兰)[2]

1 (Department of Physics, Shandong University, Jinan 250100, China)
2 (Department of Physics, Qufu Normal University, Qufu 273165, China)

Abstract We carry out a systematic study of the different contributions to the deviations of the elliptic flows from the quark number scaling in high energy heavy ion collision in a quark combination model. The effects that we considered are: the resonance decay, the flavor dependence of the quark elliptic flow and the combination of quarks/antiquarks with slightly different transverse momenta. Our results show that the deviations observed in experiments can be well reproduced within the combination framework if all the three effects are considered. We make a detailed analysis of the different contributions using a Monte-Carlo program and suggest measuring the quark number scaling in intermediate p_T range more precisely.

Key words elliptic flow, the quark number scaling, quark combination model, mass hierarchy

PACS 25.75.-q, 25.75.Ld, 12.40.-y

1 Introduction

The elliptic flow is one of the most important observables in ultra-relativistic heavy ion collisions. It carries a great deal of information not only about the initial state of the dense matter but also on the hadronization process[1—4]. The elliptic flow v_2 for a particle is defined as the coefficient of the $\cos 2\phi$-term in the Fourier expansion of the invariant differential cross section $E\mathrm{d}^3\sigma/\mathrm{d}^3p$, where ϕ is the azimuthal angle of the hadron momentum in the transverse plane[5, 6]. One of the highlights in the first few years' run of RHIC, the relativistic heavy ion collider at BNL, is the discovery of quark number scaling (QNS) of v_2 for different hadrons produced in the collisions. The discovery was one of the main reasons which led people to propose that quark combination is the dominant mechanism for hadronization of quarks and antiquarks in a dense quark matter such as a quark-gluon plasma (QGP).

The quark number scaling (QNS) observed at intermediate transverse momenta p_T at RHIC shows that, when both v_2 and p_T rescaled by the constituent quark number of the hadron, the elliptic flow is an universal function of p_T for all hadrons, which is just the corresponding elliptic flow of the quark or antiquark before hadronization. However, the recent high accuracy measurements and more abundant data at low p_T show that QNS seems not to be valid in this p_T region. Instead, there is an obviously different structure in the data, referred as the mass hierarchy[7] or fine structure of elliptic flows. This has attracted much attention[8—12] and seems to support in particular the hydrodynamic models where the mass hierarchy arises naturally from radial flows which are hadron mass dependent[8, 9].

On the other hand, it is well-known that in the coalescence/recombination models, there are a number of effects that can influence the hadron elliptic flows and lead to the deviation from QNS. The most well-known are: the resonance decay[13—15], the flavor dependence of the elliptic flow for quarks before hadronization[16—21] and the combination of quarks/antiquarks with slightly different transverse momenta[13, 19—21]. Qualitative discussions and some quantitative estimations have been given. The results seem to suggest that they can indeed account for at least partly the violation of QNS. However, the influences of these effects on the fine structure of elliptic flows have not been studied systematically in the combination-like models. It is thus unclear whether the fine structure can be explained quanti-

Received 7 August 2007, Revised 26 September 2007
* Supported by National Natural Science Foundation of China (10475049, 10775089)
1) E-mail: yt@sdu.edu.cn

tatively within the combination framework by taking these effects into account. It is also unclear which effect is more responsible for the deviations in which region, for which hadrons and in which directions.

In this paper, we make such a detailed study by taking all the three effects into account in a systematic way. We will carry out the study by using a Monte-Carlo program which is convenient in particular to investigate the decay effect systematically. The Monte-Carlo program is designed purposely for quark combination models where the initial state properties are simply taken as inputs extracted empirically from the data. We organize the study in three steps, which we will denote as three quark combination schemes in the following of this paper. In the first step, we consider only the combination of quarks/antiquarks with equal p_T but taking the production and decay of the resonances into account. This step is aimed at a detailed study of the influence from resonance decay. In the second step, we still consider only the combination with equal p_T but take the resonance decay as well as a flavor dependence of the elliptic flow of the quarks $v_{2,q}$ (p_T) into account. In this step, we will see that how the flavor dependence of $v_{2,q}$ (p_T) manifests itself in v_2 (p_T) of the final hadrons. Finally, in the third step, we take the combination of the quarks/antiquarks with unequal p_T into account to see whether we can reproduce the mass hierarchy of elliptic flows in a quark combination model by considering all these three effects together.

The content of the paper is organized as follows. In Sec. 2, we will briefly describe the quark combination model that we use for this study. In Sec. 3, we present the results for the studies in the three steps mentioned above and make discussions. Finally, a short summary is given in Sec. 4.

2 Quark combination model

In all kinds of coalescence/recombination/combination models, a quark combination rule is needed to determine which quark(s) and/or antiquark(s) to combine into a hadron. In the quark combination model (QCM) proposed some time ago[22—33], this combination rule is given by the "near correlation in rapidity" which demands that quark(s) and/or antiquark(s) that are the nearest neighbors in rapidity axis combine into a hadron. It has been shown that[23, 24] such a demand is in agreement with the fundamental requirement of QCD and uniquely determines the quark combination rule in the hadronization process. The QCM has been successfully applied to electron-positron annihilation and proton-proton/antiproton collisions[23—29]. Recently, it has also been extended to the haronization of the quark and antiquark system produced in high energy heavy ion collisions[34—36]. A Monte-Carlo program has been constructed to calculate the properties of the hadrons produced in the hadronization process while the properties of the quarks and antiquarks before hadronization are taken as inputs. This model has successfully described the global properties of the hadrons such as hadron multiplicities, p_T spectra and rapidity distribution[34—36].

Since the model is particularly designed for describing the hadronization in the quark combination scheme, it is suitable and convenient for us to use it to study the influences of the effects mentioned in last section on the elliptic flows of the hadrons. Hence we just choose to use this Mente-Carlo model for the proposed study on the fine structure of the elliptic flows of the final hadrons. We note in particular that a good agreement has been obtained between the calculations in the model and the data for multiplicities, p_T spectra and rapidity distribution by adjusting the necessary parameters. This is also important for making a realistic study of the above-mentioned effects on elliptic flows of the hadrons. In this QCM, the production of the resonances is considered systematically. The initially produced hadrons include all the hadrons with orbital angular momentum $L = 0$ hadrons, i.e. 56-plet baryons and 36-plet mesons. The resonance decay is treated by using the decay subroutine in the event generator PYTHIA[37]. All the decay channels are considered where the branch ratios are taken from the Review of particle properties.

3 The fine structure of $v_2(p_T)$ in QCM

In this section, we pay special attention to the low p_T region where the elliptic flow data for various hadrons show non-trivial fine structure. The elliptic flows as inputs for antiquarks are taken as the same as those for quarks with the same flavor. We also neglect the influence of hadron re-scattering on $v_2(p_T)$ in our study. We now present the results and conclusions obtained in the three steps (schemes) in the following.

3.1 Naive combination scheme

This is the simplest combination scheme. Here, only the quarks and/or antiquarks with equal p_T are considered to combine into a hadron and all u, d and s quarks have the same elliptic flow. With this scheme, we can study the decay effect on elliptic flows explicitly. We would not like to study the different contributions to elliptic flows from different resonances, which has been discussed in Refs. [13, 14] by considering some dominant decay channels. Here we focus on the global contributions to the fine structure from all resonances of 56-plets baryons and 36-plets mesons covering all available decay channels. To describe $v_2(p_{\rm T})$ for hadrons, we need an input of the elliptic flow for quarks $v_{2,{\rm q}}(p_{\rm T})$. A parametrization of $v_{2,{\rm q}}(p_{\rm T})$ is given in Ref. [13] as

$$v^{(0)}_{2,{\rm q}}(p_{\rm T}) = 0.078\tanh(1.59p_{\rm T}-0.27) \tag{1}$$

by fitting the data available at that time for stable hadrons other than pions. Hereafter $p_{\rm T}$ is taken in unit of GeV. We find out that, to fit the more precise data now available by taking the resonance decay into account particularly in the low $p_{\rm T}$ range, this parametrization has to be modified. We take it as the following,

$$v_{2,{\rm q}}(p_{\rm T}) = \begin{cases} 0.256p_{\rm T}^3, & 0\leqslant p_{\rm T}\leqslant 0.365, \\ 0.078\tanh[1.45(p_{\rm T}-0.25)], & p_{\rm T}>0.365\,. \end{cases} \tag{2}$$

We fix the parameters by fitting the $v_2(p_{\rm T})$ data[7] for antiproton where the decay contributions are taken into account. We adopt the power function at low $p_{\rm T}$ which is consistent to data and the expected quadratic behavior[11, 38]. Note that considering the continuity of the Eq. (2), we use the $p^3_{\rm T}$ instead of the $p^2_{\rm T}$ form. The difference resulting from the two function forms at small $p_{\rm T}$ can be neglected for the coefficient of $p^3_{\rm T}$ or $p^2_{\rm T}$ is adjustable. Fig. 1 shows the different elliptic flows as a function of $p_{\rm T}$ for final state antiproton from different parametrization forms of Eqs. (1) and (2). We see that the data for antiproton are well reproduced at small $p_{\rm T}$ with the input of Eq. (2) but the difference between the $v_2(p_{\rm T})$ obtained with the input of Eq. (1) and the data is large in this $p_{\rm T}$ region.

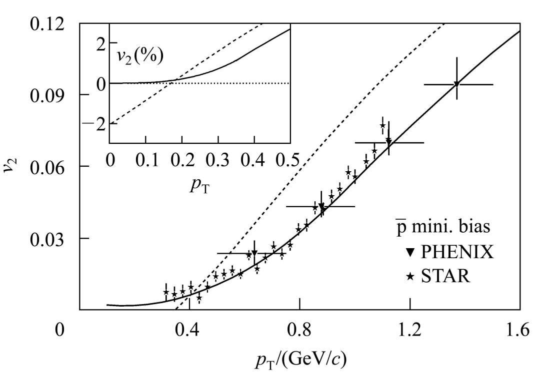

Fig. 1. v_2 vs. $p_{\rm T}$ for final state antiproton obtained in the naive combination scheme using $v_{2,{\rm q}}(p_{\rm T})$ given by Eq. (1) (dashed line) and (2) (solid line). The sub-diagram shows curves of Eq. (1) (dashed line) and (2) (solid line). The data are taken from Refs. [7, 39].

We calculate the elliptic flows for directly produced and final state hadrons using $v_{2,{\rm q}}(p_{\rm T})$ given by Eq. (2). The results are shown in Fig. 2. Here and in the following calculations, we choose the rapidity range $y\in[-0.5, 0.5]$ for hadrons to be consistent with the data. In the naive combination scheme that we are considering, the directly produced mesons have the same elliptic flows $v_{2,{\rm M}}(p_{\rm T}) = 2v_{2,{\rm q}}(p_{\rm T}/2)$ and the primary baryons have the same elliptic flows $v_{2,{\rm B}}(p_{\rm T}) = 3v_{2,{\rm q}}(p_{\rm T}/3)$, regardless of their masses and species. Comparing the upper with lower panels of Fig. 2, one observes that the decay effect obviously manifests itself at low $p_{\rm T}$. The $v_2(p_{\rm T})$ curve for the hadron i shifts to the left when the resonance decay is taken into account and the displacement depends on how much the decay contributes to the hadron i. This means that, the decay effect makes the elliptic flows of all hadrons become larger, but the enlargements are different for different hadrons. This leads to an obvious structure of $v_2(p_{\rm T})$ for hadrons in the low $p_{\rm T}$ range. We see in particular that the order of the curves for $v_2(p_{\rm T})$ of different hadrons in Fig. 2 is exactly the same as that of the data points. This shows that the decay contributions to the fine structure of elliptic flows are indeed in the right direction as observed in experiments. However, they are not enough to account for the data for all hadrons.

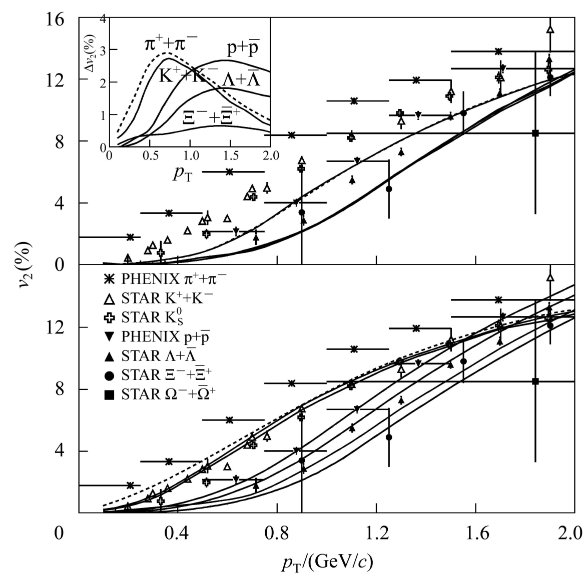

Fig. 2. v_2 vs. $p_{\rm T}$ for directly produced (upper panel) and final state (lower panel) hadrons obtained in the naive combination scheme using $v_{2,{\rm q}}(p_{\rm T})$ given by Eq. (2). The left and right curves are for the primary mesons and baryons respectively in the upper panel. The differences of $v_2(p_{\rm T})$ between upper and lower panel for various hadrons are given in the inset. The data are taken from Refs. [7, 39—41]. Note that the order of curves in the lower panel for different hadrons and those in Figs. 3 and 5 are the same as that of the data.

To see the decay contributions to $v_2(p_{\rm T})$ for different hadrons more clearly, we plot the differences of $v_2(p_{\mathrm{T}})$ between primary and final hadrons in the inset of Fig. 2. We see that the differences are small for very small or large p_{T}, because elliptic flows for hadrons approach zero as p_{T} decreases to zero or become saturated in intermediate p_{T} range. But they are quite significant in the p_{T} range where the fine structure of $v_2(p_{\mathrm{T}})$ is observed. We also see that not only the decay contributions to pions, but also these to $\mathrm{K}^+ + \mathrm{K}^-$, $\mathrm{p}+\overline{\mathrm{p}}$ and $\Lambda+\overline{\Lambda}$ are all quite significant in the p_{T} region around 1 GeV.

In this step, we see that the decay effects on the mass hierarchy are important but they are not enough to reproduce the data for all hadrons. one has to take other effects into account.

3.2 Modified naive combination scheme

Because the mass of strange quarks is different from that of u, d quarks, the p_{T} distribution and $v_{2,\mathrm{q}}(p_{\mathrm{T}})$ can also be different[18, 19, 36]. This difference can further influence the fine structure of $v_2(p_{\mathrm{T}})$ for hadrons. To study this effect, we use a "modified naive combination scheme". Here, we still only consider the combination of quarks/antiquarks with equal p_{T}, but take into account the mass effect of constituent quarks on the elliptic flows. The mass or flavor dependence of $v_{2,\mathrm{q}}(p_{\mathrm{T}})$ is a priori unknown and can not be derived from the first principle. On the other hand, we should not take it arbitrarily because it has to be constrained by the known empirical facts. Since this dependence comes from the difference of the quark mass of different flavor, we choose to use the following form determined by the heuristic arguments given below.

The modified $v_{2,\mathrm{q}}(p_{\mathrm{T}})$ for quarks is taken as

$$v_{2,\mathrm{i}}(p_{\mathrm{T}}) = \begin{cases} 0.256(p_{\mathrm{T}}/\alpha_{\mathrm{i}})^3, & 0 \leqslant p_{\mathrm{T}}/\alpha_{\mathrm{i}} \leqslant 0.365, \\ 0.078\tanh[1.45(p_{\mathrm{T}}/\alpha_{\mathrm{i}}-0.25)], & \\ p_{\mathrm{T}}/\alpha_{\mathrm{i}} > 0.365, & \end{cases} \tag{3}$$

where i=u, d or s. We let the parameter α_{i} satisfy $\alpha_{\mathrm{u}} : \alpha_{\mathrm{d}} : \alpha_{\mathrm{s}} = \langle E\rangle_{\mathrm{u}} : \langle E\rangle_{\mathrm{d}} : \langle E\rangle_{\mathrm{s}}$ at RHIC energies, and further normalize $\langle E\rangle_{\mathrm{i}}$ by $\overline{\langle E\rangle}_{\mathrm{q}} = (\langle E\rangle_{\mathrm{u}} + \langle E\rangle_{\mathrm{d}} + \langle E\rangle_{\mathrm{s}})/3$. Then the relative weight $\alpha_{\mathrm{i}} = \langle E\rangle_{\mathrm{i}}/\overline{\langle E\rangle}_{\mathrm{q}}$ obeys the normalized condition $\alpha_{\mathrm{u}}+\alpha_{\mathrm{d}}+\alpha_{\mathrm{s}}=3$. We calculate the average value of quark energies by

$$\langle E\rangle_{\mathrm{i}} = \int_0^{\infty} E_{\mathrm{i}} g(p)\mathrm{d}^3p \Big/ \int_0^{\infty} g(p)\mathrm{d}^3p \ . \tag{4}$$

If the momentum distribution is taken as a factorized form $g(p) \sim f(p_{\mathrm{T}})f_y(y)$ and the distribution of rapidity y is independent of quark flavors, then

$$\langle E\rangle_{\mathrm{i}} = A\frac{\int_0^{\infty}\sqrt{m_{\mathrm{i}}^2+p_{\mathrm{T}}^2}\,f(p_{\mathrm{T}})\mathrm{d}p_{\mathrm{T}}}{\int_0^{\infty} f(p_{\mathrm{T}})\mathrm{d}p_{\mathrm{T}}} \tag{5}$$

with constituent quark mass $m_{\mathrm{u,d}}$=0.34 GeV and m_{s}=0.5 GeV. Where the p_{T} distribution $f(p_{\mathrm{T}}) = (p_{\mathrm{T}}^{2.3}+p_{\mathrm{T}}^{0.2}+1)^{-3.0}$ is from Ref. [34], constant

$$A = \frac{\int_{-y_0}^{y_0}\cosh(y)f_y(y)\mathrm{d}y}{\int_{-y_0}^{y_0} f_y(y)\mathrm{d}y} \tag{6}$$

and parameter y_0 is the boundary of rapidity for quarks. Then the normalized relative weight $\alpha_{\mathrm{u,d}} \approx 0.94$ and $\alpha_{\mathrm{s}} \approx 1.12$ are obtained.

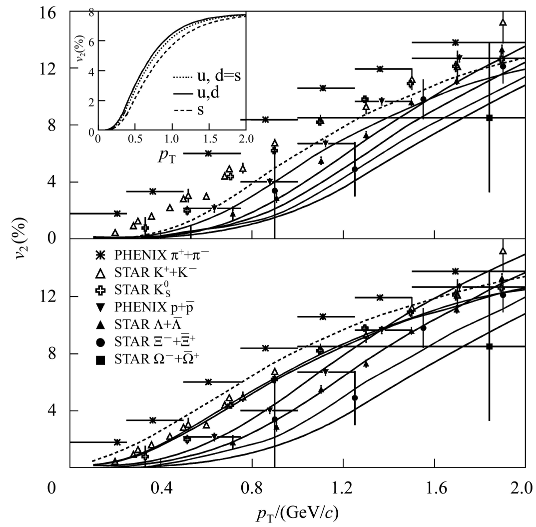

Fig. 3. v_2 vs. p_{T} for directly produced (upper panel) and final state (lower panel) hadrons obtained in the modified naive combination scheme using $v_{2,\mathrm{q}}(p_{\mathrm{T}})$ given by Eq. (3). The sub-diagram in the upper panel shows curves of Eq. (2) (dotted line) and Eq. (3) for u, d quarks (solid line) and for s quarks (dashed line). The data are taken from the same references as Fig. 2.

One sees that in the sub-diagram of Fig. 3, the mass effect makes $v_{2,\mathrm{q}}(p_{\mathrm{T}})$ bigger for u, d quarks and smaller for s quarks in low p_{T} range, but little change of $v_{2,\mathrm{q}}(p_{\mathrm{T}})$ for quarks in intermediate p_{T} region due to the elliptic flow saturation from the form of Eq. (2). The effect will further be transferred into hadrons formed and result in the dispersion of the $v_2(p_{\mathrm{T}})$ for primary hadrons. Based on the input for quark elliptic flows in Eq. (3), $v_2(p_{\mathrm{T}})$ for directly produced meson and baryon are given by

$$v_{2,\mathrm{M}}(p_{\mathrm{T}}) \approx v_{2,\mathrm{i}}(p_{\mathrm{T}}/2)+v_{2,\mathrm{j}}(p_{\mathrm{T}}/2), \tag{7}$$

$$v_{2,\mathrm{B}}(p_{\mathrm{T}}) \approx v_{2,\mathrm{i}}(p_{\mathrm{T}}/3)+v_{2,\mathrm{j}}(p_{\mathrm{T}}/3)+v_{2,\mathrm{k}}(p_{\mathrm{T}}/3), \tag{8}$$

where i, j denote the constituent quarks in the meson M and i, j, k denote those in the baryon B. Therefore the $v_2(p_{\mathrm{T}})$ for primary hadrons with the same flavor content are identical but can be different if the flavor content is different.

The results in this combination scheme are shown in Fig. 3. Comparing with Fig. 2, the $v_2(p_T)$ curves for directly produced hadrons split according to their flavor contents and this leads to even larger splittings for final state hadrons. We see a reasonable agreement between theoretical calculations and data is achieved for all the hadrons except for pions. The pion $v_2(p_T)$ is partially improved but still not enough to match the data. If we tune $\alpha_{u,d}$ to a smaller value, we would make the $v_2(p_T)$ for pions fit the data, but this would destroy the agreement with data for other hadrons. In contrast to the hydro-model interpretation of the differences among hadron $v_2(p_T)$ as hadron mass effect, the mass effect at the quark level is partially responsible for such differences in the quark combination picture. We also see that a better way to identify the mass effect of s quarks relative to u/d quarks is to study the difference between $v_2(p_T)$ for ϕ and that for K^* in experiments.

3.3 Unequal p_T combination scheme

As discussed in the coalescence/recombination models[19, 42, 43], hadron production should be determined by the overlap of parton distributions with the wave functions of formed hadrons. Quarks and/or antiquarks with different transverse momenta can also combine into a hadron. This can further affect the fine structure of elliptic flows. So we investigate this effect in this step by using an "unequal p_T combination scheme". For simplicity, we consider only a special case where, as in the previous two schemes, only collinear quarks and/or antiquarks can combine into a hadron, but their magnitudes of p_T can be different which are chosen randomly according to the quark p_T-distribution $f(p_T)$ mentioned above[34]. However, the influence from the hadron wave function on the probability for quarks/antiquarks with different p_T to combine into hadrons is difficult to determine since the wave function is unknown. Fortunately, we find out that, in the low and intermediate p_T region considered, for a given p_T of hadron, although we choose the quark transverse momentum $p_{T,i}$ randomly according to the distribution function $f(p_{T,i})$ for the partons in the system under the constraint $\sum_i p_{T,i} = p_T$, the obtained $p_{T,i}$ is not large when transformed to the rest frame of the hadron produced. This is because $f(p_{T,i})$ drops very fast with increasing $p_{T,i}$ and $\prod_i f(p_{T,i})$ at $\sum_i p_{T,i} = p_T$ takes the maximum for equal $p_{T,i}$. In the upper panel of Fig. 4, we show the distribution of quark transverse momenta in the rest frames of formed hadrons. We see that the distribution is quite narrow, whose width is about 0.35 GeV for baryons and 0.27 GeV for mesons. They are smaller than the intrinsic p_T of the quarks in hadrons. In such a narrow p_T region, we just neglect the influence from the hadron wave function by taking it as a constant. This is similar to Refs. [19, 44].

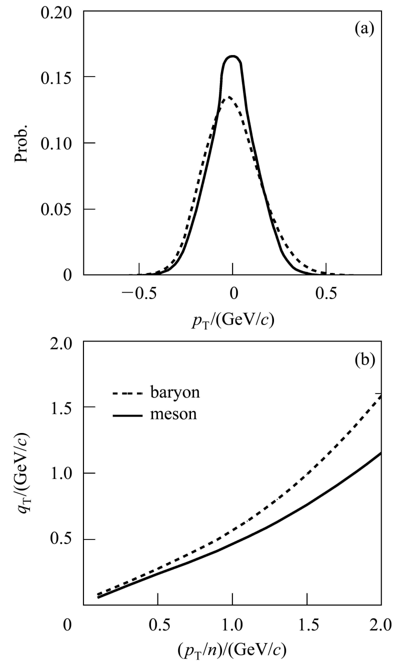

Fig. 4. (a) the distributions of quark transverse momenta for mesons (solid line) and baryons (dashed line) in the rest frames of formed hadrons in unequal p_T combination scheme; (b) q_T vs. p_T/n for mesons and baryons in the same combination scheme.

Since the combination condition is changed, we need to re-adjust the parameters in the form of $v_{2,q}(p_T)$ for quarks to fit the data of $v_2(p_T)$ for hadrons. Now it is given by

$$v_{2,q}(p_T) = \begin{cases} 0.286 p_T^4, & 0 \leqslant p_T \leqslant 0.525, \\ 0.11 \tanh[1.6(p_T - 0.4)], & p_T > 0.525, \end{cases} \tag{9}$$

whose continuity is also considered. The mass effect is introduced in the same way as Subsection 3.2. The results of (scaled) $v_2(p_T)$ for final hadrons are shown in Fig. 5. The primary hadrons with the same flavor contents also have an identical $v_2(p_T)$ curve because the combination condition of random p_T is independent of quark flavors. One sees in the upper panel that the pion $v_2(p_T)$ agrees with data very well besides other hadrons. Obviously the fine structure of $v_2(p_T)$ at low p_T is a joint effect of resonance decay, the quark mass difference in $v_{2,q}(p_T)$ and unequal p_T combination.

We see in particular that the contribution to the fine structure from unequal p_T combination is explicitly different from that of resonance decay or quark flavor dependence of $v_{2,q}(p_T)$. It splits the scaled

$v_2(p_T)$ curves for hadrons into meson and baryon two groups, because the degrees of spoiling the QNS for mesons and baryons are different in unequal p_T combination (see the lower panel of Fig. 5). This effect expands further the structure of $v_2(p_T)$ for hadrons and leads to a better agreement with the data including pions in the low p_T range. While in intermediate p_T region, the two group splitting, which is remarkably different from equal p_T combination, is more apparent and little disturbed from the other two factors. However, the splitting of two groups is still within the error bars of the data now available. More accurate data are needed to see whether this is true. Since this notable difference at intermediate p_T is little influenced by other effects, it can be taken as a criteria to judge whether unequal p_T combination contributes significantly in hadronization process.

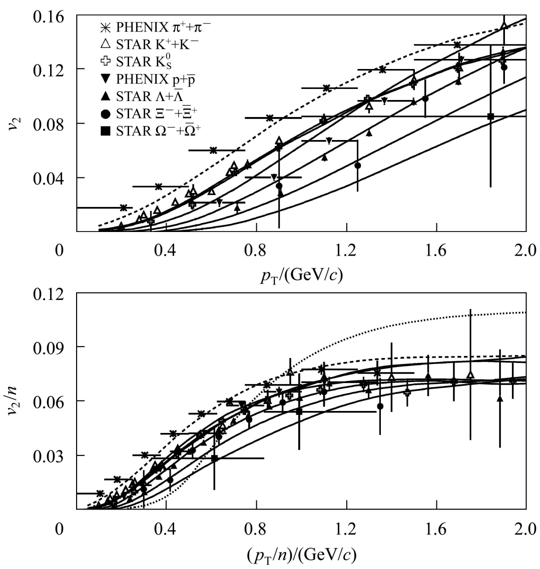

Fig. 5. The results obtained in the unequal p_T combination scheme. v_2 vs. p_T for final hadrons are given in the upper panel. v_2 scaled by constituent quark number n as a function of p_T/n for final hadrons are given in the lower panel. The dotted line is Eq. (9), the $v_{2,q}(p_T)$ for quarks inputted. The data are taken from the same references as Fig. 2.

It is clear to see in the lower panel of Fig. 5 that unequal p_T combination results in obviously violation of the QNS. To study the violation in more detail, we calculate in lab frame the average transverse momentum difference of quarks defined as

$$q_T = \left(\sum_{i=1}^{n} |p_{T,i} - p_T/n| \right) /n \ ,$$

where $p_{T,i}$'s are the transverse momenta for constituent quarks, p_T is the transverse momentum of the hadron, and n is the number of constituent quarks in the hadron. The value of q_T is a measure of the deviation of quark transverse momentum from the quark number scaled p_T of the hadron in the lab frame. The results are shown in the lower panel of Fig. 4. One sees that q_T increases with p_T/n monotonically and q_T for baryons is larger than that for mesons.

Considering a meson with p_T/n=2 GeV, according to the inputted function of $v_{2,q}(p_T)$ Eq. (9) (see dotted line in lower panel of Fig. 5), we have $v_{2,q}(2+q_T) \approx v_{2,q}(2)$ and $v_{2,q}(2-q_T) < v_{2,q}(2)$, then $(v_{2,q}(2+q_T)+v_{2,q}(2-q_T))/2 < v_{2,q}(2)$. That is, the scaled $v_2(p_T)$ curves for mesons at p_T/n=2 GeV are lower than the $v_{2,q}(p_T)$ curve for quarks. The larger q_T for baryons will lead to the even lower scaled $v_2(p_T)$ curves for baryons. Note that there is another asymptote at low p_T. For example, we have $(v_{2,q}(0.2+q_T)+v_{2,q}(0.2-q_T))/2 > v_{2,q}(0.2)$ instead. Thus the scaled $v_2(p_T)$ curves for hadrons are contrarily higher than the $v_{2,q}(p_T)$ curve for quarks in low p_T range. Anyway, the deviation from the QNS for baryons is expected to be larger than that for mesons both in low and intermediate p_T range due to the larger q_T for baryons. What we should point out is the behavior of deviation from the QNS for hadrons is consistent with that shown in Fig. 4 of Ref. [13] around p_T/n=2 GeV, but is quite different in the low p_T region. The reason is that we adopt an expected positive power function of quark elliptic flow instead of the negative part of Eq. (1) at small p_T (see Fig. 1). Then the conclusion given in the same reference that the scaled hadronic elliptic flows are smaller than the quark elliptic flow is really dependent on the function of $v_{2,q}(p_T)$ for quarks inputted. In fact the scaled hadronic elliptic flows can be larger or smaller than the quark elliptic flow depending on different $v_{2,q}(p_T)$ for quarks adopted. So the behavior of violation of the QNS in unequal p_T combination is not only dependent on the average transverse momentum difference of quarks $q_T(p_T/n)$ but also on the inputted function of $v_{2,q}(p_T)$ for quarks.

Of course the feature of two group splitting at intermediate p_T is also dependent of the quark elliptic flow. However, it appears as long as the saturation range of $v_{2,q}(p_T)$ for quarks is sufficiently broad. This is supported by the experimental fact that the saturation of $v_2(p_T)$ for hadrons is observed from $p_T > 3$ GeV up to 6 GeV[45].

As a short summary of this step, we see that, the unequal p_T combination affects the fine structure of $v_2(p_T)$ in a different way from the other two effects discussed above. It splits the scaled $v_2(p_T)$ curves into meson and baryon two groups, and the effect is more apparent in the intermediate p_T range. We also find that the scaled hadronic elliptic flows obtained in unequal p_T combination can be larger or smaller than the quark elliptic flow $v_{2,q}(p_T)$ depending on the form of $v_{2,q}(p_T)$ adopted. Together with the effects of resonance decay and flavor dependence of $v_{2,q}(p_T)$, we obtain a good agreement with the data for all hadrons including pions.

4 Summary

In the quark combination model, we have made a systematic study of the contributions from resonance decay, flavor dependence of quark elliptic flow and unequal p_T combination to the mass hierarchy of elliptic flows of the final hadrons in Au+Au collisions. Our results lead us to the following conclusions: (1) Resonance decay is indeed one of the important sources of the mass hierarchy. It contributes in the right direction as shown in the available data. However, resonance decay alone is definitely not enough to account for the observed deviations from QNS for all the different hadrons. (2) The mass effect of constituent quarks violates the QNS further and leads to a better agreement with data for hadrons but still not enough to get a good fit to pions. (3) Unequal p_T combination leads also to deviation from QNS for the produced hadrons. The deviation can be in different direction depending on the shape of $v_{2,q}(p_T)$. (4) The three effects all lead to violation of the QNS. The first two manifest themselves mainly at low p_T, while the violation from the unequal p_T combination is more apparent in intermediate p_T range. (5) By taking all the three effects into account, we have reproduced the fine structure of elliptic flows for hadrons including pions in the low p_T-region. Further prediction is given which can be used to test the combination picture by future experiments.

The authors thank Shi-Yuan Li and Zong-Guo Si for helpful discussions. Special thanks go to Zuo-Tang Liang and Qun Wang for critically reading the manuscript with many suggestions.

References

1 Ollitrault J Y. Phys. Rev. D, 1992, **46**: 229
2 Sorge H. Phys. Rev. Lett., 1999, **82**: 2048. arXiv:nucl-th/9812057
3 Barrette J et al. (E877 Collaboration). Phys. Rev. Lett., 1994, **73**: 2532. arXiv:hep-ex/9405003
4 Appelshauser H et al. (NA49 Collaboration). Phys. Rev. Lett., 1998, **80**: 4136. arXiv:nucl-ex/9711001
5 Voloshin S, ZHANG Y. Z. Phys. C, 1996, **70**: 665. arXiv:hep-ph/9407282
6 Poskanzer A M, Voloshin S A. Phys. Rev. C, 1998, **58**: 1671. arXiv:nucl-ex/9805001
7 Adams J et al. (STAR Collaboration). Phys. Rev. C, 2005, **72**: 014904. arXiv:nucl-ex/0409033
8 Huovinen P, Kolb P F, Heinz U W et al. Phys. Lett. B, 2001, **503**: 58. arXiv:hep-ph/0101136
9 Borghini N, Ollitrault J Y. Phys. Lett. B, 2006, **642**: 227. arXiv:nucl-th/0506045
10 LIN Z W, Ko C M, LI B A et al. Phys. Rev. C, 2005, **72**: 064901. arXiv:nucl-th/0411110
11 Molnar D. arXiv:nucl-th/0408044
12 Pratt S, Pal S. Nucl. Phys. A, 2005, **749**: 268; Phys. Rev. C, 2005, **71**: 014905. arXiv:nucl-th/0409038
13 Greco V, Ko C M. Phys. Rev. C, 2004, **70**: 024901. arXiv:nucl-th/0402020
14 DONG X, Esumi S, Sorensen P et al. Phys. Lett. B, 2004, **597**: 328. arXiv:nucl-th/0403030
15 Nonaka C, Muller B, Asakawa M et al. Phys. Rev. C, 2004, **69**: 031902. arXiv:nucl-th/0312081
16 LIN Z W, Ko C M. Phys. Rev. Lett., 2002, **89**: 202302. arXiv:nucl-th/0207014
17 Molnar D, Voloshin S A. Phys. Rev. Lett., 2003, **91**: 092301. arXiv:nucl-th/0302014
18 Nonaka C, Fries R J, Bass S A. Phys. Lett. B, 2004, **583**: 73. arXiv:nucl-th/0308051
19 Greco V, Ko C M, Levai P. Phys. Rev. C, 2003, **68**: 034904. arXiv:nucl-th/0305024
20 Fries R J, Muller B, Nonaka C et al. Phys. Rev. C, 2003, **68**: 044902. arXiv:nucl-th/0306027
21 LIN Z W, Molnar D. Phys. Rev. C, 2003, **68**: 044901. arXiv:nucl-th/0304045
22 XIE Q B, LIANG Z T. In: Jinan 1987, Proceedings, Multiparticle Production. Edited by Hwa R C, XIE Q B. Singapore: World Scientific, 1987. 469—496
23 XIE Q B, LIU X M. Phys. Rev. D, 1988, **38**: 2169
24 XIE Q B. In: 19th International Symposium on Multiparticle Dynamics 1988. Edited by Schiff D, Tran J Thanh Van. Singapore: France and World Scientific, 1988. 369—375
25 WANG Q, XIE Q B. J. Phys. G, 1995, **21**: 897
26 LIANG Z T, XIE Q B. Phys. Rev. D, 1991, **43**: 751
27 ZHAO J Q et al. Sci. Sin. A, 1995, **38**: 1474
28 WANG Q et al. Int. J. Mod. Phys. A, 1996, **11**: 5203
29 SI Z G et al. Commun. Theor. Phys., 1997, **28**: 85
30 WANG Q et al. Phys. Lett. B, 1996, **388**: 346
31 WANG Q, XIE Q B. Phys. Rev. D, 1995, **52**: 1469
32 WANG Q, Gustafson G, XIE Q B. Phys. Rev. D, 2000, **62**: 054004. arXiv:hep-ph/9912310
33 WANG Q, Gustafson G, JIN Y et al. Phys. Rev. D, 2001, **64**: 012006. arXiv:hep-ph/0011362
34 SHAO F L, XIE Q B, WANG Q. Phys. Rev. C, 2005, **71**: 044903. arXiv:nucl-th/0409018
35 SHAO F L, YAO T, XIE Q B. Phys. Rev. C, 2007, **75**: 034904. arXiv:nucl-th/0611026
36 SONG J, SHAO F L, XIE Q B et al. arXiv:nucl-th/0703095
37 Sjostrand T, Eden P, Friberg C et al. Comput. Phys. Commun., 2001, **135**: 238. arXiv:hep-ph/0010017
38 Danielewicz P. Phys. Rev. C, 1995, **51**: 716. arXiv:nucl-th/9408018
39 Adler S S et al. (PHENIX Collaboration). Phys. Rev. Lett., 2003, **91**: 182301. arXiv:nucl-ex/0305013
40 Adams J et al. (STAR Collaboration). Phys. Rev. Lett., 2004, **92**: 052302. arXiv:nucl-ex/0306007
41 Adams J et al. (STAR Collaboration). Phys. Rev. Lett., 2005, **95**: 122301. arXiv:nucl-ex/0504022
42 Hwa R C, YANG C B. Phys. Rev. C, 2003, **67**: 034902. arXiv:nucl-th/0211010
43 Fries R J, Muller B, Nonaka C et al. Phys. Rev. Lett., 2003, **90**: 202303. arXiv:nucl-th/0301087
44 Greco V, Ko C M, Levai P. Phys. Rev. Lett., 2003, **90**: 202302. arXiv:nucl-th/0301093
45 Adler C et al. (STAR Collaboration). Phys. Rev. Lett., 2003, **90**: 032301. arXiv:nucl-ex/0206006